environmental sciences proceedings

MDPI

Proceedings

Estimation of Land Surface Temperature from the Joint Polar-orbiting Satellite System Missions: JPSS-1/NOAA-20 and JPSS-2/NOAA-21

Fatima Zahrae Rhziel, Mohammed Lahraoua and Naoufal Raissouni

National School for Applied Sciences of Tetuan, University Abdelmalek Essaadi Remote Sensing and GIS Research Unit

Abstract: The accurate estimation of Land Surface Temperature (LST) is a vital parameter in various fields, such as hydrology, meteorology, and surface energy balance analysis. This study focuses on the estimation of LST using data acquired from the Joint Polar orbiting Satellite System (JPSS) satellites, specifically JPSS-1/NOAA-20 and JPSS-2/NOAA-21. The methodology for this research centers on the utilization of the split window algorithm, a well-established and recognized technique renowned for its proficiency in extracting accurate Land Surface Temperature (LST) values from remotely sensed data. This algorithm leverages the differential behavior of thermal infrared (TIR) radiance measured in two adjacent spectral channels to estimate LST, effectively mitigating the influence of atmospheric distortions on the acquired measurements.

To establish the accuracy of the proposed approach, the coefficients of the split window algorithm were determined through linear regression analysis, utilizing a dataset generated via extensive radiative transfer modeling. The calculated LST values were subsequently compared with LST products provided by the National Oceanic and Atmospheric Administration (NOAA). The evaluation process encompassed the computation of root mean square error (RMSE) values, offering insights into the performance of the algorithm for both JPSS-1/NOAA-20 and JPSS-2/NOAA-21 missions.

LST retrieval validation with standard atmospheric simulation indicates that the JPSS-1/NOAA-20 and The JPSS-1/NOAA-21 algorithms have demonstrated an accuracy of 1.4 K in retrieval of LST with different errors. The obtained results demonstrate the potential of the split window algorithm to effectively estimate LST from JPSS satellite data. The RMSE values, 2.05 and 1.71 for JPSS-1/NOAA-20 and JPSS-2/NOAA-21, respectively, highlight the algorithm's capability to provide accurate LST estimates for different mission datasets. This research contributes to enhancing our understanding of land surface temperature dynamics using remote sensing technology and showcases the valuable insights that can be gained from JPSS missions in monitoring and studying Earth's surface processes.

Keywords: Land Surface Temperature; split window algorithm; JPSS-1/NOAA-20 and JPSS-2/NOAA-21

Citation: To be added by editorial staff during production.

Academic Editor: FirstnameLastname

Published: date

1. Introduction

Land Surface Temperature (LST) is a fundamental element within the realm of land surface dynamics, capturing the intricate interplay between the Earth's surface and the surrounding atmosphere, as well as the exchange of energy between them [1-5]. LST serves a critical role in a wide range of applications, including the modeling of evapotranspiration [6-7], the evaluation of soil moisture levels [8-10], and the exploration of climatic, hydrological, and ecological patterns [11-18]. LST is obtained from satellite data through a process that involves correcting for atmospheric influences, addressing the absorption and emission of atmospheric surface emissivity and water vapor [20-35]. LST retrieval relies on the application of the split-window technique. The development of Split-Window (SW) algorithms is rooted in variations associated with atmospheric effects and surface emissivity [19-20, 36-39].

Surface emissivity corresponds to the radiative flux of thermal radiation emitted by a surface element. It is crucial for determining the thermal radiation from the Earth's surface and is a fundamental parameter that influences the accuracy and efficiency of LST retrieval.

Hence, fluctuations in atmospheric transmittance are closely linked to the dynamics of water vapor content within the atmospheric profile for thermal channels [30]. In this paper, we compared operativity, performance and effectively from Joint Polar-orbiting Satellites JPSS-1/NOAA-20 and JPSS-2/NOAA-21 algorithms for retrieving LST NOAA data [40].

2. The radiative transfer equation role in land surface temperature estimation.

The radiative transfer equation represents a fundamental principle, used in various fields of science and engineering, including astrophysics, atmospheric science, remote sensing, and heat transfer. It describes the transport of radiant energy such as electromagnetic radiation through a medium.

The equation is particularly useful for understanding how energy is absorbed, scattered, and transmitted as it interacts with particles or substances within the medium.

In clear sky conditions, the top-of-atmosphere radiance recorded by a space-borne sensor $L_{sensor,\lambda}$ comprises the surface emission contributions, the atmospheric, upwelling and downwelling radiance $L^{\uparrow}_{atm,\lambda}$ and $L^{\downarrow}_{atm,\lambda}$ Reflected by the ground surface and altered by the atmosphere (equation 1). Retrieval algorithms depend on one or more top-of-atmosphere spectral measurements to account for atmospheric effects and estimate LST.

$$L_{sensor,\lambda} = \left[\varepsilon_\lambda B(T_S) + (1-\varepsilon_\lambda)L^{\downarrow}_{atm,\lambda}\right]\tau_\lambda + L^{\uparrow}_{atm,\lambda} \qquad (1) \qquad (1)$$

where, B(Ts) refers to the blackbody radiance as defined by Planck's law, Ts represents the Land Surface Temperature, and ε_λ stands for the land surface emissivity.

The Visible Infrared Imaging Radiometer Suite (VIIRS) LST is established through comparisons with ground-based measurements and LST products from other instruments, particularly the NOAA series of LST products.

3. LST Inversion Techniques.

Obtaining atmospheric parameters from in-situ radiosoundings and using radiative transfer is a common approach in remote sensing and atmospheric science. These atmospheric parameters are essential for correcting remote sensing data, particularly for estimating Land surface temperature accurately.

The atmospheric parameters are acquired through in situ radiosoundings and the utilization of radiative transfer codes, such as MODTRAN [41]. Equation (1) has the potential to calculate Ts by inverting Planck's law. The inversion of Equation (1) can be achieved by correcting for atmospheric and emissivity effects.

Therefore, Inverting Planck's law involves:

$$T_S = \frac{C_1}{\lambda \ln\left(\dfrac{C_2}{\lambda^5 \left(B(T_i) + L_{sensor,\lambda} - (1-\varepsilon_\lambda) L^{\downarrow}_{atm,\lambda} \right) / \tau_\lambda \varepsilon_\lambda} + 1 \right)} \quad (2)$$

where, λ is the effective band wavelength and Planck's law constants : C_1 = 14387.7 μm.K and C_2 = 1.19104*108 W.μm^4.m^{-2}.sr^{-1}.

The atmospheric parameters were derived from the Operational Vertical Sounder (TOVS) Thermodynamic Initial Guess Retrieval (TIGR3) database [42] and simulated using the MODTRAN model.

3.1. Split-Window Algorithm for Land Surface Temperature estimation.

The SW algorithm is a widely used method for estimating land surface temperature (LST) on remote sensing data in the thermal infrared region and depends on the differential absorption characteristics of two thermal infrared channels.

The SW algorithm applies quadratic combination of brightness temperatures to calculate LST [42]. It estimates LST by exploiting the distinct atmospheric absorptions in two adjacent thermal infrared spectral regions, assuming known emissivity. SW algorithm coefficients are sensitive affected by changing total column water vapor (WVC) and various viewing angles [25], [27], [43].

The SW algorithm has been widely used by researchers to retrieve both sea surface temperature (SST) and land surface temperature (LST) from remote sensing data. In this paper, the two-channel algorithm proposed by [39] has been used, which takes into account the emissivity and water vapor effects.

The formula of the SW algorithm is as follows:

$$T_s = T_i + c_1 (T_i - T_j) + c_2 (T_i - T_j)^2 + c_0 + (c_3 + c_4 W)(1-\varepsilon) + (c_5 + c_6 W)\Delta\varepsilon \quad (3)$$

In this formula, Ts represents the surface temperature (in Kelvin), T_i and T_j are the brightness temperatures from different thermal channels (in Kelvin), ε is the mean effective emissivity, Δε is the emissivity difference, w is the total atmospheric water vapor (in grams per square centimeter), and c_0 to c_6 denote the SW coefficients.

4. MODTRAN for Simulating Atmospheric Parameters.

The atmospherics parameters determination is through simulations that account for local atmospheric conditions, particularly water vapor content. These simulations establish the relationship between atmospheric transmittance and water vapor content and are conducted using atmospheric modeling software like MODTRAN (MODerate spectral resolution atmospheric TRANsmission). MODTRAN is widely employed in the fields of remote sensing and atmospheric research to calculate anticipated brightness temperatures for specific thermal channels on JPSS-1/NOAA-20 and JPSS-2/NOAA-21 satellites. MODTRAN serves as a well-established tool for modeling the radiative transfer of electromagnetic radiation through Earth's atmosphere.

Temperature profiles were meticulously derived from radiosoundings, originating from the Television InfraRed Observation Satellite (TIROS) Operational Vertical Sounder (TOVS) Thermodynamic Initial Guess Retrieval (TIGR3) database [42]. These calculations spanned a wide spectrum of temperature gradients.

Furthermore, the calculations encompassed various viewing angles, a comprehensive range of atmospheric water vapor values, and 100 distinct emissivity values obtained from spectral responses of diverse surface types available in the Advanced Spaceborne Thermal Emission Reflection Radiometer (ASTER) spectral library [44].

The MODTRAN outputs provide essential atmospheric parameter values: atmospheric transmittances, atmospheric upwelling and downwelling radiances. These values are acquired through mathematical convolution employing two filter functions that correspond to the thermal infrared channels of the JPSS-1/NOAA-20 and JPSS-2/NOAA-21 satellites.

5. Numerical Coefficients and Sensitivity Analysis

The SW algorithm coefficients refer to the parameters used in the SW algorithm for estimating LST from TIR remote sensing satellite. These coefficients are crucial for the algorithm as they are used in the mathematical equations to convert the observed radiance values into LST values.

The coefficients in Equation 1 were calculated through the minimization of simulations from a constructed database for the JPSS-1/NOAA-20 and JPSS-2/NOAA-21 satellites.

To assess the influence of individual error sources on the SW algorithm, a sensitivity analysis was conducted. This analysis aimed to evaluate the algorithm's performance across a range of meteorological conditions and land cover types:

$$\delta_{\text{Total}}(T_s) = \sqrt{\delta_{\text{alg}}^2 + \delta_{\text{NE}\Delta\text{E}}^2 + \delta_{\varepsilon}^2 + \delta_{\text{W}}^2} \quad (4)$$

the total error in LST calculated from elementary errors: the algorithm standard deviation, the impact of uncertainties in at-sensor temperatures, land surface emissivity, and atmospheric water vapor.

6. Analysis of split-window algorithm coefficients and sensitivity results.

Sensitivity analysis, which includes factors such as land surface emissivity, channel noise, water vapor, is a crucial element in the assessment of the performance and precision of LST retrieval algorithms.

The SW coefficients present in Table 1 were obtained from regressions methods for the JPSS-1/NOAA-20 and JPSS-2/NOAA-21 satellites.

Table 1. JPSS-1/NOAA-20 and JPSS-2/NOAA-21 Satellites: Split-Window Algorithm Coefficients.

Satellites	C_0	C_1	C_2	C_3	C_4	C_5	C_6
NOAA-11	0.021	1.878	0.268	57.2	0.07	-132	10.31
NOAA-12	0.030	1.623	0.306	57.1	-0.08	-135	12.12
JPSS-1/NOAA-20	-0.16	1.330	0.230	58.1	-0.57	-112	8.84
JPSS-2/NOAA-21	0.079	1.297	0.216	58.6	-0.62	-99	5.88

Table 2 illustrates the impact of minimization errors for JPSS-1/NOAA-20 and JPSS-2/NOAA-21 in Kelvin (K). The respective values are 1.09 K and 1.07 K, with corresponding correlation coefficients (R) of 0.91 and 0.93. Additionally, there are noise-induced errors of 0.23 K and 0.22 K, as well as errors attributed to atmospheric water vapor content uncertainty, which amount to 0.04 K and 0.02 K.

When accounting for a 1% uncertainty in surface emissivity, the LST total error is 1.75 K and 1.67 K for JPSS-1/NOAA-20 and JPSS-2/NOAA-21, respectively. If the surface emissivity uncertainty is reduced to 0.05%, the total error becomes 1.30 K and 1.26 K for the two respective satellites.

Table 2. The sensitivity analysis of impacting factors for JPSS-1/NOAA-20 and JPSS-2/NOAA-21.

Satellite	R	δ_{alg} (K)	$\delta_{NE\Delta T}$ (K)	δ_{ε} (1%)	δ_{ε} (0.5%)	δ_{W} (K)	$\delta_{Total}(T_s)$ (1%)	$\delta_{Total}(T_s)$ (0.5%)
NOAA-11	0.96	1.04	0.29	1.57	0.79	0.03	1.91	1.34
NOAA-12	0.94	1.06	0.28	1.56	0.78	0.06	1.91	1.35
JPSS-1/NOAA-20	0.91	1.09	0.23	1.35	0.67	0.04	1.75	1.30
JPSS-2/NOAA-21	0.93	1.07	0.22	1.26	0.63	0.02	1.67	1.26

7. Split-Window algorithms Validation.

Validation methods are essential for assessing whether Land Surface Temperature (LST) data conforms to specified standards or accuracy requirements. Ground-based validation is a common approach that involves comparing remote sensing-derived LST values with measurements collected on the ground. This method has been widely employed to validate LST products.

Sensitivity analysis serves to evaluate the impact of potential errors the SW algorithm retrieval. Additionally, validation is imperative to discover the algorithm's alignment with real-world LST values. In this study, two distinct validation methods were employed: standard atmospheric simulations and ground truth datasets supplied by [45].

Table 3. Geolocation and surface type of the two sites.

Site location	Altitude	Longitude	Surface type
Walpeup, northwest of Melbourne	35°12'S	142°36'E	Cropland
Hay, new south Wales	23°24'S	145°18'E	Vegetation / soil mixture

Two homogeneous surface sites located in Australia were used for LST validation; their geolocation and surface type are presented in Table 3. The mean emissivity was given by Prata in [45] of 0.98 for both sites.

The AD592 solid-state temperature transducers were employed to perform in situ temperature measurements at both sites. Detailed information about the functioning of these devices is provided by [46].

Table 4 presents the validation for NOAA algorithm series in comparison to the ground truth dataset. The last column of the table provides the RMSE values for the algorithms when applied to the total data acquired at sites, Hay and Walpeup.

Table 4. SW algorithms Validation using ground truth datasets.

Sensor	Mean differences (bias) (K)	Standard deviation of differences (K)	Root Mean Square Error (K)
NOAA-11	0,74	1,37	1,87
NOAA-12	0,77	1,33	1,77
JPSS-1/NOAA-20	1,10	1,43	2.05
JPSS-1/NOAA-21	0.97	1.31	1.71

The results demonstrate the successful derivation of LST NOAA series by these algorithms, characterized by mean difference values of 1.10 K for JPSS-1/NOAA-20 and 0.97 K for JPSS-2/NOAA-21, respectively. Additionally, these algorithms yield LST data with a standard deviation of approximately 2.05 K for JPSS-1/NOAA-20 and less than 1.71 K for JPSS-2/NOAA-21 at both the Hay and Walpeup sites.

The analysis results demonstrate the SW capability to generate LST RMSE values ranging between 1.61 K and 1.96 K for the Hay and Walpeup locations (NOAA11 dataset) and between 1.71 K and 2.05 K for the Hay and Walpeup locations (NOAA12 dataset). Furthermore, Figure 1 shows a good matching between the NOAA-20 and NOAA-21 retrieved LSTs and the measured ones with a correlation coefficient of 0.98.

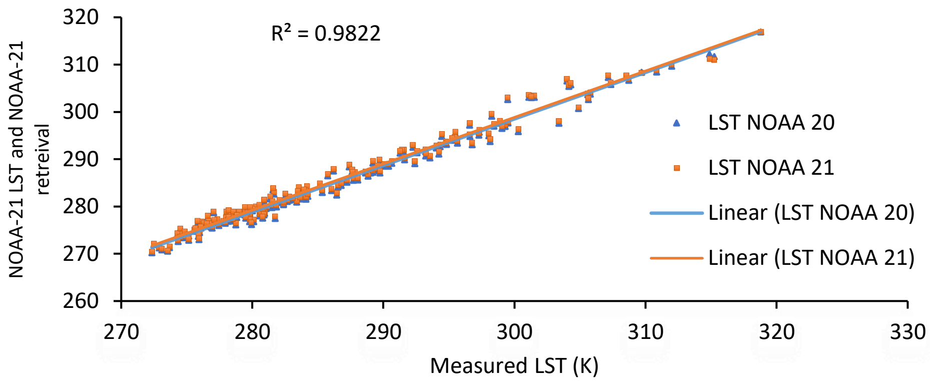

Figure 1. Validation of NOAA-21 and NOAA-20 split window algorithm using the ground truth data set of [45].

The satisfactory performance of the JPSS algorithms during the validation process, utilizing datasets, underscores the algorithm's capability to deliver precise Land Surface Temperature (LST) estimations under well-defined atmospherics transmittances, grounds emissivity, and atmospherics waters vapors conditions. The accuracy of algorithms, establishes this as a favorable choice for applications involving the retrieval of LST from VIIRS sattelites data.

8. Conclusion

The JPSS-1/NOAA-20 and The JPSS-1/NOAA-21 algorithms are used to retrieve LST in this study. The algorithms coefficients were obtained from the atmospheric profiles dataset simulation. The ground data was used to evaluate the algorithms.

The validation and comparison using the ground truth data sets from two Australian sites, confirm JPSS algorithms performances. Basing to the RMSE of the retrieved LSTs from the measured data, the algorithms are very powerful in its LST calculation. The accuracy of LST retrieval is compared to that NOAA-11 and 12. The algorithms have a higher accuracy with the ground truth data set for NOAA-11 and 12 with precise in situ atmospheric water vapor contents. The Sensitivity analysis validation, shows the accuracy with 1.4 K in LST retrieval for the JPSS-1/NOAA-20 and The JPSS-1/NOAA-21 algorithms. The accuracy of these algorithms is about 1.71 K and 2.05 for the ground truth dataset.

References

1. Anderson, M.; Norman, J.; Kustas, W.; Houborg, R.; Starks, P.; Agam, N. A thermal-based remote sensing technique for routine mapping of land-surface carbon, water and energy fluxes from field to regional scales. Remote Sens. Environ. 2008, 112, 4227–4241.
2. Mannstein, H. Surface Energy Budget, Surface Temperature and Thermal Inertia. In Remote Sensing Applications in Meteorology and Climatology; Vaughan, R.A., Ed.; Springer Netherlands: Dordrecht, The Netherlands, 1987; pp. 391–410.
3. Sellers, P.; Hall, F.; Asrar, G.; Strebel, D.; Murphy, R. The first ISLSCP field experiment (FIFE). Bull. Am. Meteorol. Soc. 1988, 69, 22–27.
4. G. R. Diak and M. S. Whipple. "Improvements to models and methods for evaluating the land-surface energy balance and effective roughness using radiosonde reports and satellite-measured skin temperature data. Agr Forest Meteorol. 1993, 63, 189–218.
5. Anderson, M.; Norman, J.; Kustas, W.; Houborg, R.; Starks, P.; Agam, N. A thermal-based remote sensing technique for routine mapping of land-surface carbon, water and energy fluxes from field to regional scales. Remote Sens. Environ. 2008, 112, 4227–4241.
6. Brunsell, N.A.; Gillies, R.R. Length scale analysis of surface energy fluxes derived from remote sensing. J. Hydrometeorol. 2003, 4, 1212–1219.
7. Olioso, A.; Chauki, H.; Couraul, D.; Wigneron, J. P. Estimation of evapotranspiration and photosynthesis by assimilation of remote sensing data into SVAT models. Remote Sens. Environ. 1999, 68, 341–356.
8. Chehbouni, A.; Lo Seen, D.; joku, E. G.; onteny, B. A. Examination of the difference between radiative and aerodynamic surface temperatures over sparsely vegetated surfaces. Remote Sens. Environ. 1996, 58, 177–186.
9. Schmugge, T. J. Remote sensing of surface soil moisture. J. Appl. Meteorol. Climatol. 1978, 17, 1557–1978.

10. Price, J. C. The potential of Remotely Sensed Thermal Infrared data to Infer Surface Soil Moisture and Evaporation. Water Resour. 1990, 16, 787–795.
11. Santanello, J.; Peters-Lidard, C. D.; Garcia, M. E.; Mocko, D. M.; Tischler, M. A.; Moran, M. S.; Thoma, D. P. Using remotely-sensed estimates of soil moisture to infer soil texture and hydraulic properties across a semi-arid watershed. Remote Sens. Environ. 2007, 110, 79–97.
12. Schmugge, T.J.; André, J.-C. Land Surface Evaporation: Measurement and Parameterization; Springer: New York, NY, USA, 1991.
13. Arnfield, A.J. Two decades of urban climate research: A review of turbulence, exchanges of energy and water, and the urban heat island. Int. J. Climatol. 2003, 23, 1–26.
14. Hansen, J.; Ruedy, R.; Sato, M.; Lo, K. Global surface temperature change. Rev. Geophys. 2010, 48.
15. Parkinson, C.L.; Greenstone, R.; Closs, J. EOS Data Products Handbook. Volume 2; NASA Goddard Space Flight Center: Greenbelt, MD, USA, 2000.
16. Oyoshi, K.; Akatsuka, S.; Takeuchi, W.; Sobue, S. Hourly LST Monitoring with Japanese Geostationary Satellite MTSAT-1R over the Asia-Pacific Region. Asian J. Geoinform. 2014, 14, 1–13.
17. S. W. Running. C. Justice. V. Salomonson. D. Hall. J. Barker. Y. Kaufman. A. Strahler. A. Huete. Muller, J.-P.; Vanderbilt, V.; Wan, Z.; Eillet, P. Terrestrial remote sensing science and algorithms planned for EOS/MODIS. Int. J. Remote Sens. 1994, 17, 3587–3620.
18. Li, Z.; Liu, W. z.; Zhang, X. c.; Zheng, F. l. Impacts of land use change and climate variability on hydrology in an agricultural catchment on the Loess Plateau of China. J. Hydrol. 2009. 377. 35–42.
19. [31] Fisher, J. B.; Tu, K. P.; Baldocchi, D. D. Global estimates of the land-atmosphere water flux based on monthly AVHRR and ISLSCP-II data. validated at 16 FLUXNET sites. Remote Sens. Environ. 2008, 112, 901–919.
20. Becker, F.; Li, Z.L. Toward a local split window method over land surface. Int. J. Remote Sens. 1990 a, 11, 369–393.
21. Becker, F.; Li, Z.-L. Surface temperature and emissivity at various scales: Definition, measurement and related problems. Remote Sens. Rev. 1995, 12, 225–253.
22. Sobrino, J.A.; Li, Z.; Stoll, M.P.; Becker, F. Multi-channel and multi-angle algorithms for estimating sea and land surface temperature with ATSR data. Int. J. Remote Sens. 1996, 17, 2089–2114.
23. François, C.; Ottlé, C. Atmospheric corrections in the thermal infrared: Global and water vapor dependent split-window algorithms-applications to ATSR and AVHRR data. IEEE Trans. Geosci. Remote Sens. 1996, 34, 457–470.
24. Sobrino, J.A.; El Kharraz, J.; Li, Z.-L. Surface temperature and water vapour retrieval from MODIS data. Int. J. Remote Sens. 2003, 24, 5161–5182.
25. Becker, F.; Li, Z.L. Temperature-independent spectral indices in TIR bands. Remote Sens. Environ, 1990 b, 32, 17–33.
26. Li, Z.-L.; Becker, F. Feasibility of land surface temerature and emissivity determination from AVHRR data. Remote Sens. Environ. 1993, 43, 67–85.
27. Sobrino, J.A.; Li, Z.-L.; Stoll, M.P.; Becker, F. Improvements in the split-window technique for land surface temperature determination. IEEE Trans. Geosci. Remote Sens. 1994, 32, 243–253.
28. Valor, E.; Caselles, V. Mapping land surface emissivity from NDVI: Application to European, African, and South American areas. Remote Sens. Environ. 1996, 57, 167–184.
29. Wan, Z. ; Li, Z.-L. J. A physics-based algorithm for retrieving land surface emissivity and temperature from EOS/MODIS data. IEEE Trans. Geosci. Remote Sens. 1996, 35, 980–996.
30. Sobrino, J.A.; Raissouni, N. Toward remote sensing methods for land cover dynamic monitoring: Application to Morocco. Int. J. Remote Sens. 2000, 21, 353–366.
31. Sobrino, J.A.; Raissouni, N.; Li, Z. A Comparative Study of Land Surface Emissivity Retrieval from NOAA Data. Remote Sens. Environ. 2001, 75, 256–266.
32. Li, J.; Li, Z.; Jin, X.; Schmit, T.J.; Zhou, L.; Goldberg, M.D. Land surface emissivity from high temporal resolution geostationary infrared imager radiances: Methodology and simulation studies. J. Geophys. Res. 2011, 116.
33. Li, Z.; Li, J.; Li, Y.; Zhang, Y.; Schmit, T.J.; Zhou, L.; Goldberg, M.D.; Menzel, W.P. Determining diurnal variations of land surface emissivity from geostationary satellites. J. Geophys. Res. 2012, 117.
34. Masiello, G.; Serio, C. Simultaneous physical retrieval of surface emissivity spectrum and atmospheric parameters from infrared atmospheric sounder interferometer spectral radiances. Appl. Opt. 2013, 52, 2428–2446.
35. Masiello, G.; Serio, C.; Venafra, S.; Liuzzi, G.; Göttsche, F.; Trigo, I.; Watts, P. Kalman filter physical retrieval of surface emissivity and temperature from SEVIRI infrared channels: A validation and intercomparison study. Atmos. Meas. Tech. 2015, 8, 2981–2997.
36. 8. Prata, A.J. Land surface temperatures derived from the AVHRR and the ATSR, 2, Experimental results and validation of AVHRR algorithms. J. Geophys. Res. 1994, 99, 13025–13058.
37. Sobrino, J.A.; Li, Z.-L.; Stoll, M.P.; Becker, F. Improvements in the split-window technique for land surface temperature determination. IEEE Trans. Geosci. Remote Sens. 1994, 32, 243–253.
38. 9. Price, J.C. Land surface temperature measurements from the split window channels of the NOAA-7/AVHRR. J. Geophys. Res. 1984, 89, 7231–7237.
39. 10. Wan, Z.; Dozier, J. Ageneralized split-window algorithm for retrieving land-surface temperature measurement from space. IEEE Trans. Geosci. Remote Sens. 1996, 34, 892–905.

40. JPSS LSTWebsite. Available online: https://www.star.nesdis.noaa.gov/jpss/lst.php.
41. Berk, A.; Anderson, G. P.; Acharya, P. K.; Chetwynd, J. H.; Bernstein, L. S.; Shettle, E. P. Matthew, M. W.;Adler-Golden, S. M. MODTRAN 4 user's manual, MA: Air Force Research Laboratory. Space Vehicles Directorate. Air Force Materiel Command. Hascom AFB. 1999.
42. Scott, N. A.; Chedin, A. A fast line by line method for atmospheric absorption computations. J. Meteorol. 1981, 20, 802–812.
43. Wan, Z.; Dozier, J. A generalized split-window algorithm for retrieving land-surface temperature from space. IEEE Trans. Geosci. Remote Sens. 1996, 34, 892–905.
44. Hook, S. J. The ASTER Spectral Library. Pasadena. CA: Jet Propulsion Lab. online: http://speclib.jpl.nasa.gov/ 1999.
45. Prata, A.J. Land surface temperatures derived from the AVHRR and the ATSR, 2, Experimental results and validation of AVHRR algorithms. J. Geophys. Res. 1994, 99, 13025–13058.
46. Prata, A. J., Validation data for land surface temperature determination. CSIRO Tech. Memo., CSIRO, Div. of Atmos. Res., Aspendale, Australia. In press., 1994b